Resonance Characteristics in Offshore Wind Power Plants with 66 kV Collection Grids

IOP Conf. Series: Journal of Physics: Conf. Series **1356** (2019) 012025 doi:10.1088/1742-6596/1356/1/012025

Resonance Characteristics in Offshore Wind Power Plants with 66 kV Collection Grids

A Holdyk[1, 3], Ł H Kocewiak[2]

[1] SINTEF Energy Research, Trondheim, Norway
[2] Ørsted Wind Power, Gentofte, Denmark

andrzej.holdyk@sintef.no

Abstract. This paper presents a study of the influence of doubling the collection grid voltage on the electric resonances in the collection grid of large offshore wind power plants. This was done using wide-band models of most important passive components such as transformers and cables. Wide-band models based on measurements (black box) of transformers were used. Scaling of admittance matrix elements was used in order to adjust the voltage ratio of the measured wind turbine transformers to take into account the doubled voltage at the medium voltage side.

It was shown that doubling the collection grid voltage decreases the main resonance frequency seen at the medium voltage terminal of the wind turbine transformers as well as the offshore substation transformer. The decrease was approximately 25 per cent when doubling the voltage and keeping the same number of turbines in a radial. When the number of turbines was doubled, there was a proportional decrease of the resonance frequency.

Decreasing the main resonance frequency in offshore wind power plants might have an impact on the harmonic and transient behaviour and should therefore be investigated by developers.

***Index Terms*—harmonics, offshore wind power plants, resonance, wide-band models.**

1. Introduction

Nowadays, large offshore wind power plants (WPPs) are characterized by a complex electrical infrastructure comprising of number of wind turbines (WTs) with step-up transformers, offshore transformers and wide spread offshore array collection cable grid which is typically connected to the grid via HVAC transmission cables. Such a system creates challenges in analysis and design covering harmonic propagation and transient studies. Typically used voltage level of collection grids of large OWPPs is approximately 33 kV. Doubling it might provide technical or economic benefits; therefore, it is foreseen that a part of the large offshore WPPs in the future will be at 66 kV level. This change might influence the harmonic and transient behaviour of OWPPs as compared to those known today. It is

[3] This work was supported by the Norwegian Research Centre for Offshore Wind Technology (Nowitech). https://www.sintef.no/projectweb/nowitech/.

therefore important to analyse how the increase of the collection grid voltage level changes the electrical environment characteristic of an offshore WPP in a wide frequency range. In this study, focus is put on a passive part of the collection grid, i.e. the WT converter and its control are not considered.

Section 2 presents procedures and methods used to generate wide-band models of cables and transformers. Section 3 presents results of studies performed on the wide-band model of a WPP. Discussion of the main factors influencing the main resonance frequencies in the collection grids of OWPPs is presented in section 4 and section 5 summarizes the findings and concludes the paper.

2. Wide-band model of offshore WPP

2.1. Transformers

There is a limited choice of accurate transformer models if the representation of wide-band characteristic is needed. So-called white models can represent wide-band characteristic but require detailed information of transformer construction and are known often not to be very precise at higher frequencies. On the other hand, black-box models are based on admittance matrix measurements of a transformer and, if performed correctly, can be very accurate in the wide-band of frequencies, especially at medium and high frequencies.

In this study, we use wide-band black-box model based on admittance measurements of WT and WPP offshore transformers performed during Ph.D. projects [1, 2]. Transformers for 66 kV collection grids were not available at the time of the measurement campaign, therefore, mathematical manipulation is used to change the wide-band characteristic of transformers build for 33 kV collection grid into those for 66 kV collection grids.

2.1.1. Measurements.

The black-box model of a transformer is based on a short-circuit admittance matrix measurements of a transformer in a wide band of frequencies. Here, a sweep frequency response analyser (SFRA) was used for that purpose. The detailed procedure of how to use a SFRA device to measure the admittance matrix of a transformer is provided in [3].

2.1.2. Positive Sequence Impedance at Lower Frequencies

Black-box models based on admittance measurements might suffer from low accuracy at lower frequencies due to several reasons, such as precision of a measurement system measuring very small impedances and measurement system internal impedance [3]. To check the precision of the measured admittance matrix, a standard T-equivalent representation of the transformer was developed based on manufacturer's data and compared with measurements. A diagram of the T-equivalent transformer model is shown in Figure 1

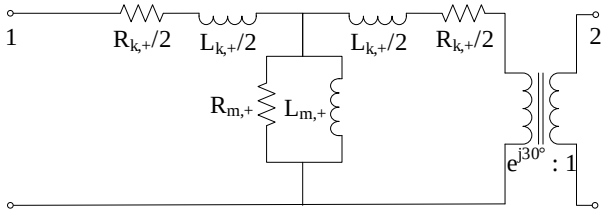

Figure 1 T-equivalent model of transformer

The positive sequence impedance matrix, Z_+ was calculated based on the manufacturer's data and T-equivalent:

$$Z_+(\omega) = \begin{bmatrix} 0.5 \cdot Z_{SC}(\omega) + Z_{OC}(\omega) & \frac{Z_{OC}(\omega)}{a} \\ \frac{Z_{OC}(\omega)}{a} & \frac{0.5 \cdot Z_{SC}(\omega) \cdot a^2 + Z_{OC}(\omega)}{a^2} \end{bmatrix} \quad (1)$$

$$Z_{SC}(\omega) = R_k + j\omega L_k \tag{2}$$

$$Z_{OC}(\omega) = \frac{1}{Y_{OC}} \tag{3}$$

$$Y_{OC}(\omega) = \frac{1}{R_m} + \frac{1}{j\omega L_m} \tag{4}$$

The positive sequence admittance matrix is calculated as:

$$Y_+(\omega) = \frac{1}{Z_+(\omega)} \tag{5}$$

A comparison of admittance matrix elements of the measured and calculated models for the WPP transformer is shown below in Figure 2. The measured and calculated elements of admittance matrix are in close agreements in all frequencies below 3 kHz. Therefore, the measured admittance matrix was used in the study without additional corrective measures.

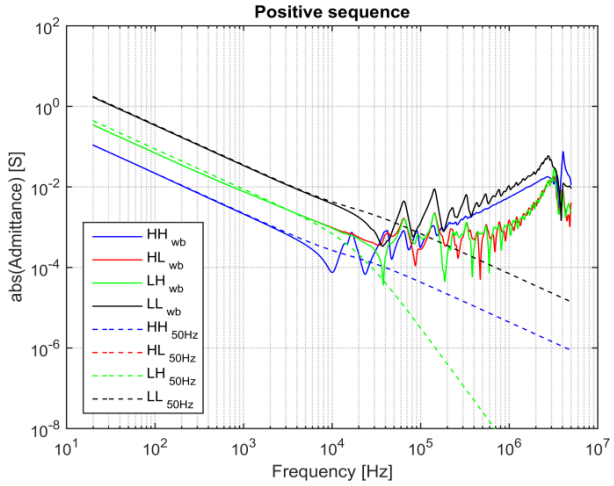

Figure 2 Comparison of magnitude of positive sequence admittance matrix elements of measured (wide-band, WB) and calculated (50 Hz) models

2.1.3. Changing voltage ratio.

The admittance matrix of WT and WPP offshore transformers were scaled in order to change voltage ratio to account for the doubled collection grid voltage. This scaling method does not influence resonance frequencies of a transformer, which change when a transformer structure changes.

Transformer's positive sequence voltage ratio can be calculated from the positive sequence admittance matrix as:

$$V_{HL} = -Y_{HH}^{-1}(\omega)Y_{HL}(\omega), I_L = 0 \tag{6}$$

$$V_{LH} = -Y_{LL}^{-1}(\omega)Y_{LH}(\omega), I_H = 0 \tag{7}$$

where, V_{HL} and V_{LH} are voltage ratios from high-to-low and from low-to-high, respectively. Y_{HH},Y_{HL}, Y_{LH} and Y_{LL} are admittance matrix elements.

Scaling of the admittance matrix in order to account for doubling of voltage at high voltage side is done by:

$$\begin{bmatrix} I_H(\omega) \\ I_L(\omega) \end{bmatrix} = \begin{bmatrix} \alpha^2 Y_{HH}(\omega) & \alpha Y_{HL}(\omega) \\ \alpha Y_{LH}(\omega) & Y_{LL}(\omega) \end{bmatrix} \begin{bmatrix} V_H(\omega) \\ V_L(\omega) \end{bmatrix} \tag{8}$$

Where, α is a ratio between new and old voltage level.

This procedure is used for WT transformers. Scaling of admittance matrix in order to account for doubling of voltage at low voltage side is done by:

$$\begin{bmatrix} I_H(\omega) \\ I_L(\omega) \end{bmatrix} = \begin{bmatrix} Y_{HH}(\omega) & \alpha Y_{HL}(\omega) \\ \alpha Y_{LH}(\omega) & \alpha^2 Y_{LL}(\omega) \end{bmatrix} \begin{bmatrix} V_H(\omega) \\ V_L(\omega) \end{bmatrix} \quad (9)$$

This procedure is used for the WPP offshore substation transformer.

2.2. Cables

Three cable models were assumed for the study: 500mm2 and 95mm2 at 66 kV level and 500mm2 for 33 kV. All cables are three-core submarine cables and were represented as admittance matrices. The characteristic admittance of each cable was calculated based on design (datasheet) information and cable length using MATLAB implementation of cable constants routine, similar to those used in EMT programs. The most important parameters for each cable are presented in Table 1. Each phase of the cable is made of two conductors, i.e. main conductor and a sheath. Relative permeability of conductors and ground resistivity are assumed to be 1 and 10 Ωm, respectively.

Table 1 Main modelling information of collection grid cables

Cable	Cond. No.	Inside Radius $[m]$	Outside Radius $[m]$	Resistivity $[\Omega \cdot m]$	Insulator rel. permittivity ϵ_{ins}
95 mm^2/ (66 kV)	1	0	0.0056	1.78E-08	3.17
	2	0.01580	0.01581	2.14E-07	2.30
500 mm^2 (66 kV)	1	0	0.0131	1.85E-08	3.05
	2	0.02350	0.02351	2.14E-07	2.30
500 mm^2 (33 kV)	1	0	0.0131	1.85E-08	3.11
	2	0.02250	0.02261	1.72E-08	2.30

The driving point impedance of a section of 1 km of the three modelled submarine cables is shown in Figure 3.

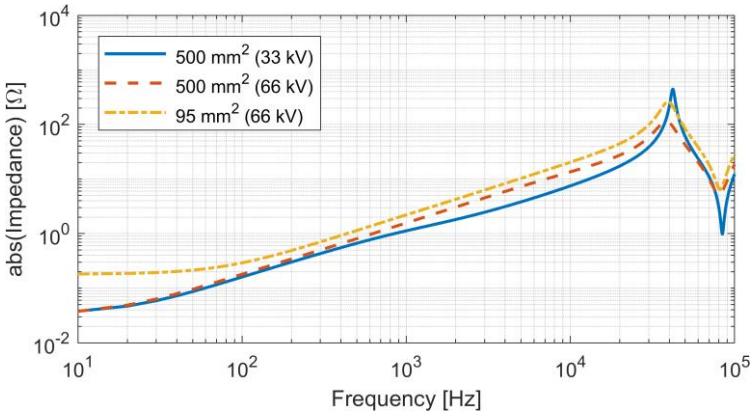

Figure 3 Driving point impedance of 1 km section of submarine cables

2.3. Wind turbines

The WT is modelled as a transformer and a small passive load (90 kW), thus the converter and filter are not represented.

2.4. External grid

The external or export grid is a high voltage (HV) grid to which the WPP is connected, usually at 132 kV, 220 kV or 400 kV level. Modelling the external grid using a lumped R and L values based on the short circuit data, as is often done for 50 Hz studies, might result in artificial resonances visible at the collection grid and therefore is usually not recommended in wide-band studies [4].

In order to model a wide-band characteristic of an external grid, a positive sequence frequency sweep was made on a 138 kV node in a PSCAD's model of IEEE's 118 bus benchmark network. The network consists of loads, capacitor banks, transmission lines and generators

3. Results

To simplify the investigation, a WPP model with a single radial is proposed. The single line diagram is shown in Figure 4:

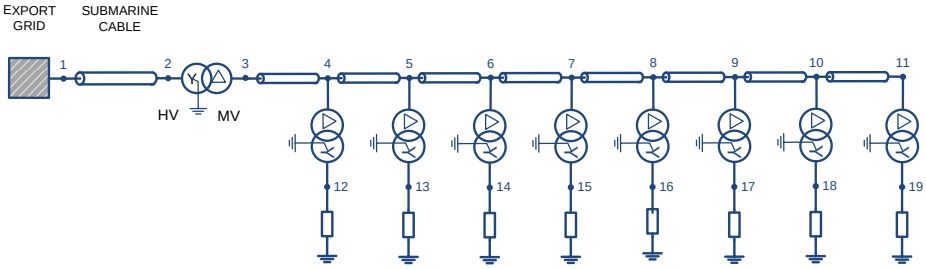

Figure 4 Structure of the investigated WPP

Two models were made with the same structure, one for 33 kV and one for 66 kV collection grid. In both cases the same number of WTs is assumed as well as the same WT sizes, thus, the 66 kV collection grid cables are of smaller cross-sections than in the 33 kV collection grid.

Models were developed in MATLAB as a frequency-dependent admittance matrix. Only positive sequence is modelled and investigated.

An additional model was developed to test a case where the number of WTs in a row is doubled at 66 kV as compared to 33 kV. Here, 16 WTs are placed in a single row instead of 8, as in the base-case described above. Such placement of WTs allows developers to double the installed capacity per radial, thus limiting the number of radials or increasing the power of a WPP significantly. Typically, the number of submarine cables going to an offshore substation is limited by physical constraints, e.g. number of J-tubes. Doubling the number of WTs increased the size of the modelled admittance matrix to 35×35×900. A simplified representation of the structure of this case with indication of the node numbering is shown in Figure 5. Two cross-sections of cables were used in the radial, the first eight WTs are connected by 500 mm^2 cables and the last eight WTs are connected by 95 mm^2.

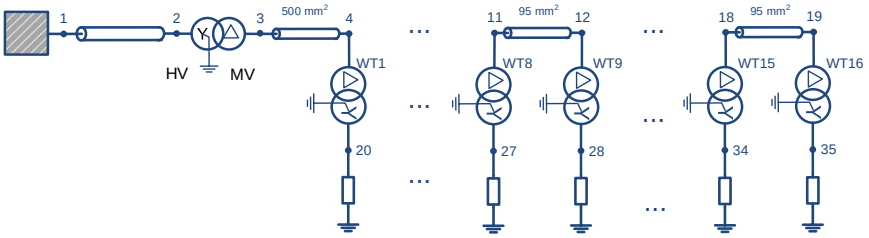

Figure 5 Structure of the investigated WPP with 16 WTs in a radial.

Driving point impedances at MV nodes of WTs for the two investigated collection grid voltages are presented in Figure 6 (next page).

The main resonance frequency (seen at node 3) for the 33 kV case is at 1479 Hz, while for 66 kV it is at 1109 Hz (8 WTs) which is 74.98% of the 33 kV resonance frequency. In the case with 16 WTs in a row, the resonance frequency is 676 Hz.

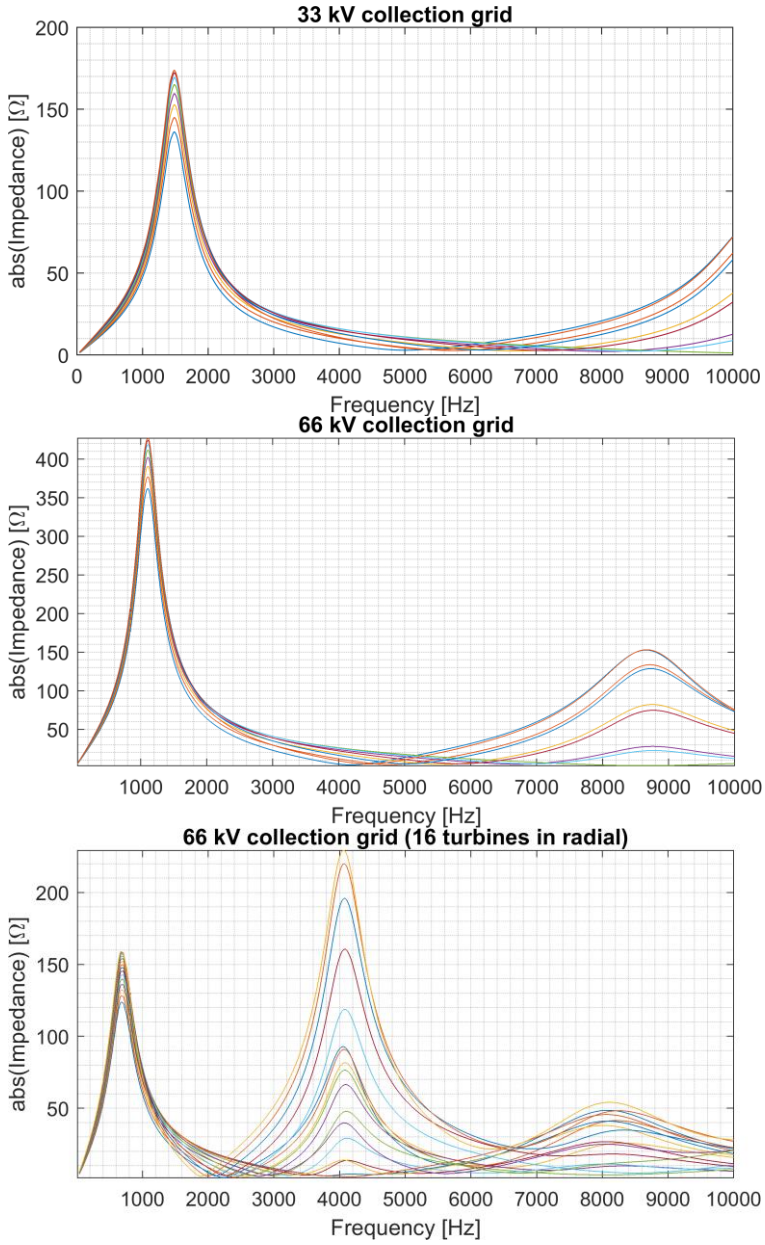

Figure 6 Driving point impedances at MV side of each WT. Up: 33 kV; middle: 66 kV (8 WTs); bottom: 66 kV (16 WTs).

3.1. Influence of WPP size

The main resonance frequency was obtained for node 3 from simulations with varied number of rows of the WPP models. The impedance of the offshore transformer was scaled to adjust its rating to the total power of WPP. All elements of the offshore transformer's admittance matrix were multiplied by constant $\beta = (\frac{P_{OWPP}}{90})$, where P_{WPP} is the total power of the WPP in MW. This was done for all WPP powers over 90 MW. Results are shown in Table 2 and in Figure 7.

Each radial is 48 MW (8 WTs) or 96 MW (16 WTs). The size of the WPP is increased by adding additional radials in parallel. Sizes up to approximately 400 MW were investigated.

Table 2 Frequency of main resonance (at node 3) in collection grid versus the size of the WPP. Each radial is 48 MW (8 WTs) or 96 MW (16 WTs). Size of the WPP is increased by adding additional radials in parallel. Each radial is 8 km long.

Total power [MW]	**Total length of MV cable [km]**	**Main resonance frequency [Hz]**		
		33 kV	**66 kV** (8 WTs / radial)	**66 kV** (16 WTs / radial)
48	8	1479	1109	-
96	16	1189	851	758
144	24	1122	812	-
192	32	1122	812	758
240	40	1084	812	-
288	48	1084	794	716
336	56	1084	794	-
384	64	1084	794	707

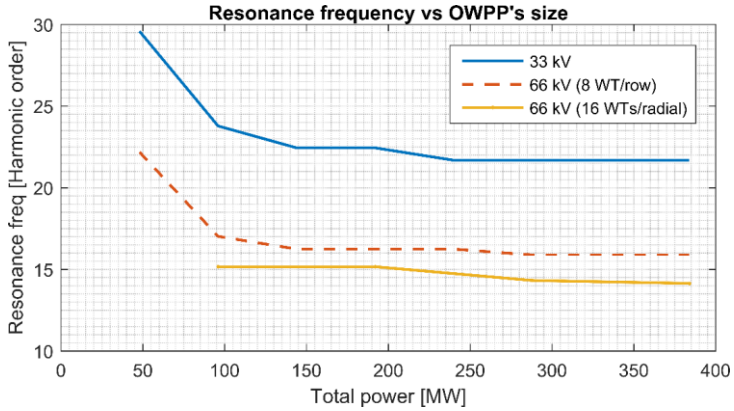

Figure 7 Frequency (in harmonic order) of main resonance in collection grid versus the size of the WPP.

It is clear that the main resonance frequency decreases when the collection grid voltage increases. The resonance frequency decreases with the increase of size of a WPP, however, the change is not significant. The initial variation visible at Figure 7 (below 100 MW) is due to the fact that the admittance of WPP offshore transformer was scaled for the WPP rated capacity above 90 MW.

4. Discussion

4.1. Main Differences in Components for 33 kV and 66 kV

Previous studies have shown that the first (main) resonance frequency in the collection grid of offshore WPP is mainly dependent on the total inductance and total capacitance of the collection grid [5, 6, 7]. Main contributors to the total inductance are transformers (leakage inductance) and main contributors to the capacitance are cables, unless there is a compensating device connected at the collection grid. Therefore, for the sake of simplicity, it is assumed the main resonance frequency is due to cables and transformers, ignoring also their resistive parts.

4.1.1. Submarine cables

The cable capacitance, C, depends mainly on the properties and dimensions of the insulation material:

$$C = \frac{2\pi\epsilon}{\ln\frac{r_{INS-outer}}{r_{INS-inner}}} \quad (10)$$

where, $r_{INS-inner}$ is the inner radius of the insulation and $r_{INS-outer}$ is the outer radius of the insulation. Cables for both investigated voltage levels use cross-linked polyethylene, or XLPE, as an insulation material; therefore, the difference in capacitance is caused by the difference in thickness of the insulation, which is increased with the voltage level. The higher the voltage level, the higher the thickness and the lower the capacitance for the same cable cross-section. We assumed 8 mm thickness for 33 kV and 9 mm thickness for 66 kV. This is shown for the four most common cable cross-sections in Figure 8

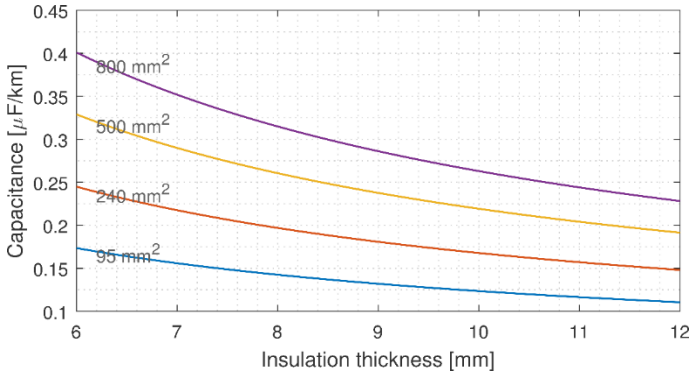

Figure 8 Capacitance for different values of insulation thickness and conductor cross sections

Figure 8 was created using equation (12) for capacitance, where:

$$r_{INS-inner} = \sqrt{\frac{A_c}{\pi}} \tag{11}$$

where, A_c is nominal area of a conductor and d_{INS} is insulation thickness. Solid conductor is assumed and semi-conductive layers are ignored.

Figure 9 shows percent difference between cable capacitance for 66 kV compared to 33 kV for conductor cross-sections between 95 mm^2 and 1200 mm^2 .

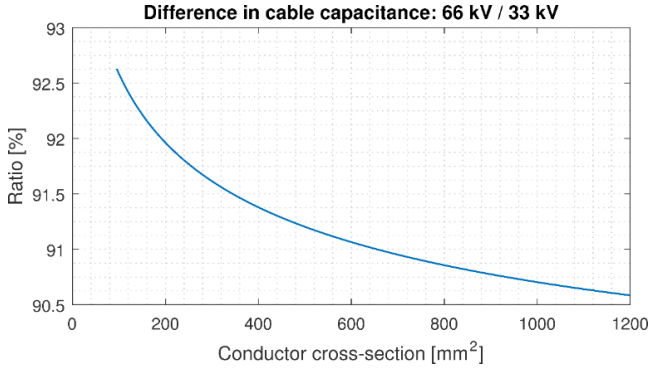

Figure 9 Percent of difference between cable capacitance for 66 kV compared to 33 kV for various conductor cross-sections.

The capacitance of 66 kV cables is lower than the capacitance of 33 kV cables for corresponding cross-sections. The larger the conductor cross-section, the larger the difference in capacitance. Cross-sections up to 1200 mm^2 were investigated and the largest difference was approximately 10%.

4.1.2. Transformers

Ignoring resistive losses, transformer's leakage inductance can be calculated as:

$$L_{SC} = \frac{Z_{SC}}{2\pi f} \tag{12}$$

$$L_{SC} = \frac{\frac{V_p^2}{S} \cdot \frac{u_k(\%)}{100}}{2\pi f} = \frac{V_p^2}{S} \cdot \frac{u_k(\%)}{100} \cdot \frac{1}{2\pi f} \tag{13}$$

where, V_p is the primary side voltage, S is transformer power, Z_{SC} is short circuit impedance and u_k (%) is percentage of short circuit voltage.

It can be easily noticed that doubling the voltage quadruples the inductance, assuming the power and percent of short circuit voltage constant. In practice, the short circuit impedance of transformers has a major effect on system fault level and depends on the system design. It determines the maximum current flow through the transformer under fault conditions.

Figure 10 shows an example of a transformer for 8 MW WT. The following transformer data is assumed: S = 9.6 MVA, ratio 33(66)/0.69 kV, u_k (%) = 6%.

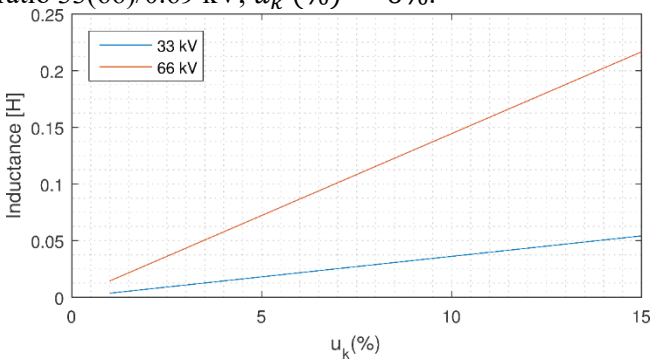

Figure 10 Leakage inductance for different values of short circuit percent voltage $u_k(\%)$ and two voltage levels.

The magnitude of short circuit impedance is a tradeoff between economics and design; therefore, manufacturers usually offer a range of impedances, e.g. 5-10 %. It can be seen in Figure 10 that shifting to 66 kV quadruples the transformer's leakage inductance (ideal case, no losses assumed). In practice, the inductance can be minimized by increasing the core cross-section or extending the length of the winding, but this will increase the weight of the transformer and might significantly increase the price as well as pose constraints to offshore application in WTs.

Therefore, increasing the voltage level of collection grid from 33 kV to 66 kV will significantly increase the total inductance in the system, thus decreasing the main resonance frequency.

4.2. Influence of scaling of admittance matrix of transformer model on its wide-band characteristics

Scaling of admittance matrix was used in order to adjust the voltage ratio of the measured WT transformers to take into account the doubled voltage at the medium voltage side. It must be stressed that the scaling did not influence the resonance frequencies of the transformer (neither in the admittance matrix elements nor in the voltage ratio), which would change in a real transformer as doubling the voltage requires a change in the winding structure which causes changes in capacitances and inductances of the winding (between turns, between winding and the core, etc.). Large transformers (in the range of several MVA) have winding resonance frequency in the kHz range, usually 2-10 kHz, therefore, the applied scaling should not have significant influence on the investigated collection grid frequency characteristic in the harmonic frequency.

4.3. Cable compensation in collection grids

Decreased capacitance and increased inductance in the collection grid means the power factor in uncompensated 66 kV collection grids should be closer to 1 than in analogous 33 kV grids. Although not investigated in the paper, this property of 66 kV collection grids should result in lower needs for additional inductive reactive compensation of cables, either dynamically by WTs or by shunt reactors.

5. Summary and conclusions

The standard voltage level of collection grids of large offshore WPPs is approximately 33 kV. Doubling it might provide technical or economic benefits; therefore, it is foreseen that a part of the large offshore WPPs in the future will be at 66 kV level. This study investigated the influence of doubling the collection grid voltage on the electric resonances in the collection grid. This was done using wide-band models of the most important passive components, i.e. transformers and cables. Wide-band models based on measurements (black box) of transformers were used. Scaling of the admittance matrix was used in order to adjust the voltage ratio of the measured WT transformers to take into account the doubled voltage at the MV side. It must be stressed that the scaling did not influence resonance frequencies of the transformer (neither in admittance matrix elements nor in the voltage ratio) which would change in a real transformer.

It was shown that doubling the collection grid voltage decreases the main resonance frequency seen at the MV terminals of WTs. The decrease was approximately 25% with doubling the voltage and keeping the same number of WT in a radial.

The main WPP resonance frequency depends mainly on the inductance of transformers and capacitance of cables. A simple study showed that with increase of voltage the capacitance of cables decreases (as the insulation thickness increases) and the inductance of transformers increases. The decrease in capacitance is below 10 %, depending on conductor size. Inductance of transformers increases with the square of the nominal voltage, i.e. it is quadrupled when voltage doubles. In practice, this value depends on the design parameters of transformers, e.g. short circuit impedance, and might be lower than quadrupled. The large increase in the total inductance in the collection grid is the main factor for the decrease of the main resonance frequencies.

6. Acknowledgments

The authors would like to express their appreciation to Troels Stybe Sørensen from Ørsted Wind Power, who supported the development of the new modelling methods.

References

[1] I. Arana, "Switching overvoltage in off-shore wind power grids. Measurements, modelling and validation in time and frequency comain," Kgs. Lyngby, Denmark, 2011.

[2] A. Holdyk, "Interactions between main electrical components in wind farms," Kgs. Lyngby, Denmark, 2014.

[3] A. Holdyk, B. Gustavsen, I. Arana and J. Holboell, "Wideband Modelling of Power Transformers Using Comercial sFRA Equipment," *IEEE Transactions on Power Delivery,* vol. 29, no. 3, pp. 1446-1453, 2014.

[4] Y. Vernay and B. Gustavsen, "Application of Frequency-Dependent Network Equivalents for EMTP Simulation of Transformer Inrush Current in LArge Networks," in *International Conference on Power Systmes Transients*, Vancouver, Canada, 2013.

[5] V. Kersiulis, A. Holdyk, J. Holboell and I. Arana, "Sensitivity of Nodal Admittances in an Offshore Wind Power Plant to Parametric Variations in the Collection Grid," in *11th International Workshop on Large-Scale Integration of Wind Power into Power Systems as well as on Transmission Netowrks for Offshore Wind Power Plants*, Lisbon, Portugal, 2011.

[6] V. Kersiulis, "M.Sc. Thesis: Sensitivity of electrical conditions in an offshore wind farms to parametric varations in collection grid cables, simulated in ATP-EMTP," Kgs. Lyngby, 2012.

[7] Ł. H. Kocewiak, B. L. Ø. Kramer, O. Holmstrøm, K. H. Jensen and L. Schuai, "Resonance damping in array cable systems by wind turbine active filtering in large offshore wind power plants," *IET Renewable Power Generation,* vol. 11, no. 7, pp. 1069-1077, 2017.